The Assessment of Mildly Aged XLPE Insulation using Polarization – Depolarization Current Measurement

Ashok Narayan Tripathi and **Supriyo Das**[†], Non-members

ABSTRACT

Insulation systems used in the power system have to interact with the environment, which leads to their aging and, eventually, failure. Cross–linked polyethylene (XLPE) insulation of underground cables is a vital component of the power system. The condition of XLPE underground cable insulation has a significant impact on the reliability and economical operation of the electrical power grid. Several techniques have been in use for the condition assessment of underground cables. The Polarization and Depolarization Current (PDC) measurement method has been commonly used to assess moisture and the aging condition of the underground cable insulation system. In this work, the dielectric response of XLPE samples, aged under different humidity and fixed temperature conditions, is investigated. The PDC measurement is carried out on unaged and aged samples. The XLPE samples are aged under constant stress and cyclic stress. The PDC-measured data are used to estimate the degradation index and loss factor. The depolarization characteristics obtained from PDC measurement are further processed to obtain equivalent electrical circuit parameters, i.e., resistance and capacitance of XLPE insulation based on the Extended Debye Model. Using model parameters, dissipation factor and ageing factor are estimated under different ageing conditions

Keywords: Polarization – Depolarization Current, XLPE, Ageing, Hamon approximation, Extended Debye Model

1. INTRODUCTION

Due to its excellent electrical, physical, and chemical properties, XLPE-insulated cables are now commonly used for the distribution system. But it cannot always retain its original structure due to aging. Most of the cable insulation failures occur because they were operated under electrical, mechanical, thermal, and environmental stress [1, 2]. With increasing operating time, the failure rate of the cables can increase exponentially. The problems arising from continuous high-voltages applications and various aging mechanisms of cable insulation may lead to degradation, which reduces the cable's service life. It affects the reliability of the power transmission network, and the result is economic loss [3]. All the degraded underground cables can be very expensive to repair and remove. Therefore, it is needed to prioritize the cables according to their severity of degradation using an effective diagnostic test method to replace only those cables, which may affect the reliability of the electrical network [4, 5].

When voltage is applied to a dielectric material, electric field distribution in the insulation volume activates various conduction and polarization mechanisms. A change in the structure of the insulation would generally lead to higher dielectric losses. Approaches based on Dielectric Response (DR) are used to investigate the change in insulation structure. DR is the memory effect of any dielectric material, and therefore can be used for insulation assessment. Insulation degradation changes the DR, and its measurement provides a picture of the insulation condition [6-8]. Non-destructive time-domain test methods such as the PDC and RVM for measuring DR have been introduced and are popular nowadays. The PDC test has been widely used to assess degradations in power transformers, high-voltage insulation systems, and machines. There is also a marked interest in recent years in using the PDC test to assess the deterioration of cable insulation [9-11]. It is reported that PDC provides very fast response at low frequencies with good accuracy. Also, it is reported that depolarization current characteristics obtained from PDC measurement provide information about the aging degree quantitatively [12, 13].

In this work, accelerated aging was performed in a thermal–humidity-controlled chamber under temperature and humidity stress. The samples are aged under constant and cyclic stress. PDC measurement is carried out on both aged and unaged XLPE cable insulation samples. From the experimental results, the degradation index and loss factor are estimated. Further, the experimental results are processed to obtain equivalent electrical circuit parameters, i.e., resistance and capacitance, using the Extended Debye Model. Using these circuit parameters, the dissipation factor and aging

Manuscript received on July 5, 2024; revised on October 9, 2024; accepted on October 22, 2024. This paper was recommended by Associate Editor Chawasak Rakpenthai.

The authors are with Department of Electrical Engineering, National Institute of Technology Jamshedpur, India.

[†]Corresponding author: supriyodas.ee@nitjsr.ac.in

Digital Object Identifier: 10.37936/ecti-eec.2525231.254886

factor are calculated.

2. EXPERIMENTAL METHODOLOGY

In this work, PDC measurement is carried out to understand the aging of XLPE cable insulation. The schematic diagram of PDC measurement is shown in Fig. 1. The cable sample is placed in a shielded box, and it is grounded. The aluminum electrodes at the two ends of the cable are grounded. The middle electrode is connected to an electrometer for measurement of current. High voltage, e.g., 1 kV DC, is applied to the cable core. According to this method, DC charging voltage (V_o) is applied to the dielectric for a certain time in order to complete all the polarization processes. During this period, the measured current consists of polarization and conduction current. After a certain period of charging, the applied DC voltage is turned off and the sample is short-circuited to ground. During this turn–off period, the current recorded is depolarization current, which no longer contains conductive current [14-16].

A single-core 33 kV XLPE with 10 mm insulation thickness is used for the experiment. The XLPE samples taken are 12 inches in length. At one end, the conductor of 1.5 inches is exposed, and this acts as the HV terminal. In the remaining portion, the semiconducting layer of 3.5 inches is stripped from both ends. The aluminum tape is wrapped around the exposed insulation and remaining semiconducting layer to form electrodes [14-16]. Fig. 2 shows the electrode configuration of XLPE samples used for PDC measurement. Fig. 3 shows the experimental setup for the PDC measurement. The PDC measurement is carried out using the KEITHLEY 6517B Electrometer. The charging voltage of 1 kV DC is applied. The duration of voltage application is varied from 0.5 to 2 hrs. The depolarization time is taken to be the same as the charging time. The bare conductor and semiconducting layer of the XLPE sample are kept shorted for at least 24 hours before taking any measurements. This is done to clear any memory effect of XLPE. While carrying out the experiments, to avoid any surface leakage current, the exposed XLPE layer from both ends is shorted and connected to the ground [15].

Aging of cable insulation is a slow degradation process due to the effect of various operating conditions such as temperature, humidity, electrical stress level, chemical effects, etc. Therefore, under normal operating conditions, ageing of cable insulation takes a long time. In the laboratory, accelerated aging is carried out to age the XLPE samples. According to accelerated aging, the applied stress level is higher than normal and is applied for a short duration [17]. In this work, a thermal and humidity–controlled chamber is used to age XLPE samples at fixed temperatures and varying RH conditions. The XLPE samples are aged under either constant stress or cyclic stress for 30 days. In constant aging, the temperature is kept at 60 ^{0}C and relative humidity is either 50% or 80%. However, in cyclic aging,

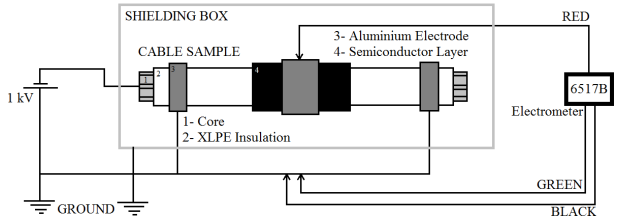

Fig. 1: Schematic diagram of the PDC measurement method.

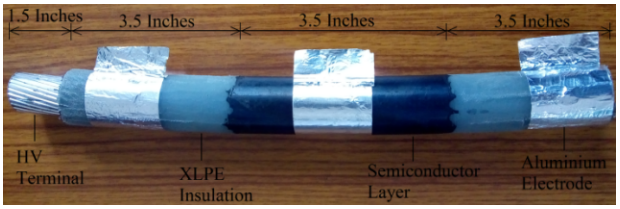

Fig. 2: Electrode configuration of XLPE sample.

in a day, for 12 hours temperature–humidity stress is applied, and for the remaining 12 hours, no stress is applied. The aging conditions and sample classifications are given in Table 1.

3. ESTIMATED AGEING PARAMETERS

The depolarization current data, obtained from PDC measurement, is used to assess the aging of XLPE. The parameters, i.e., degradation index and loss factor, are estimated from the depolarization current characteristics. Further, the depolarization current characteristics are mathematically processed to estimate parameters based on the Extended Debye model. The parameters estimated are the model parameters, dissipation factor, and aging factor.

Degradation Index

Degradation Index provides information about the aging condition and depends on the amount of polariza-

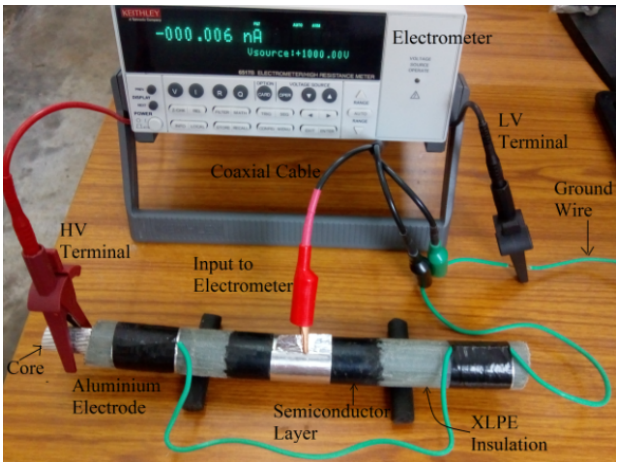

Fig. 3: Experimental Set – up.

***Table 1**: XLPE sample specifications.*

Sample Type	Stress Conditions	Ageing Type
Sample 1	Unaged XLPE	-
Sample 2	60 ℃, 50% RH	Constant stress
Sample 3	60 ℃, 80% RH	Constant stress
Sample 4	60 ℃ 50% RH	Cyclic stress
Sample 5	60 ℃ 80% RH	Cyclic stress

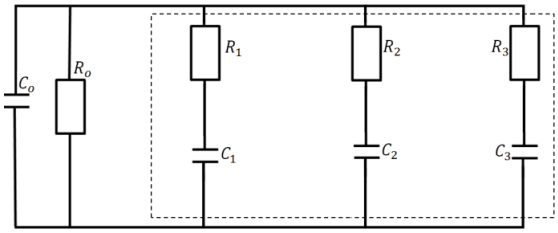

***Fig. 4**: Equivalent circuit diagram of extended Debye model.*

tion/absorption charge. It is the ratio of the absorption charge Q & C_0V_0 and is given by equation (1). The amount of absorption charge is given by equation (2) [6].

$$D_I = \frac{100Q}{C_0V_0}\% \tag{1}$$

$$Q = \int_{t_1}^{t_2} I_D(t)dt \tag{2}$$

where V_0 is the charging voltage, C_0 is the geometric capacitance of the test object, and its calculated value is 93.51 pF, $I_D(t)$ is the depolarization current, and the integration period of $I_D(t)$ is taken to be 10 secs, i.e., t_1 = 0 and t_2 = 10 secs.

Loss Factor

The loss factor gives an indication about the quality of the insulation. In this work, the loss factor is estimated in the frequency domain using the Hamon approximation. Based on the Hamon approximation, the loss factor is expressed simply by equation (3). Equation (3) indicates that the observed transient current $I_D(t)$ corresponds to frequency $f = 0.1/t$ [18, 19].

$$\epsilon_r''(f) = \frac{I_D(0.1/t)}{\omega.C_0.V_0} \tag{3}$$

where V_0 is the charging voltage, C_0 is the geometric capacitance of the test object, and its calculated value is 93.51 pF, $\omega = 2\pi f$ is the relaxation frequency.

The dielectric materials undergo different polarization and relaxation processes when subjected to applied voltage. The depolarization current characteristics comprise different relaxation processes with different time constants. To assess the aging of XLPE insulation, considering the relaxation processes, dissipation factor and aging factor are estimated based on the Extended Debye model [6, 14].

Extended Debye Model Parameters

According to this model, an RC equivalent circuit is used to analyze depolarization characteristics obtained from PDC measurement. A schematic equivalent circuit diagram of the extended Debye model is shown in Fig. 4. The equivalent circuit consists of geometrical capacitance (C_0), insulation resistance (R_0), and R–C series branches representing different relaxation phenomena and are connected in parallel. The geometric capacitance and insulation resistance are calculated using the physical dimension of the test object and conduction current characteristics, respectively. The parallel R - C branches (enclosed by a dotted line), i.e., $R_1 - C_1$, $R_2 - C_2$ and $R_3 - C_3$ or in general, $R_i - C_i$, denote exponential relaxation current components with different relaxation time constants. The curve fitting tool in MATLAB is used to estimate R and C values of the R–C series branch and optimal time constant. The equation for R_i and C_i calculation is given by (4) and (5) [20, 21].

$$R_i = V_0\left(1 - e^{\frac{t}{\tau_i}}\right)/\alpha_i \tag{4}$$

$$C_i = \tau_i/R_i \tag{5}$$

where V_0 is the charging voltage, R_i and C_i are the resistance and capacitance of the i^{th} R–C branch, τ_i is the relaxation time constant of the i^{th} R–C branch, α_i is the exponential constant of the i^{th} R–C branch.

In this work, 3 time constant is considered, which attribute to the relaxation process. It is reported in [7] that three main relaxation processes satisfactorily explain the depolarization characteristics of XLPE insulation. The relaxation processes are insulation bulk polarization, interfacial polarization in the amorphous and crystalline interfaces, and polarization of metal and salt hydrated ions due to humidity aging or presence of the water. The 3 time constants are represented by 3 R–C parallel branches. The first branch corresponds to insulation bulk polarization, the second branch represents interfacial polarization, and the third branch relates to the polarization of metal salt hydrated ions.

To obtain optimal time constant values and to estimate extended Debye model parameters, a curve-fitting technique is used. The curve fitting of depolarization characteristics is carried out using the MATLAB toolbox. In the curve fitting technique, the Levenberg –Marquardt algorithm (LMA) along with the bi-square weight method for robust fitness is used. In order to obtain optimal parameters with the least uncertainties, the method of fixed time constants is used [22]. Therefore, the time constant values are varied using trial and error within the range of 10^{-2} to 10^4 s. This time constant range is considered as it is reported in [23] that in the case of XLPE, within this range boundary, interfacial polarization occurs and may contribute to ions wandering and

surface and space charge accumulation. In addition, R-squared (determination coefficient) is used as a criterion to assess the goodness of fit. With an R-squared value more than 0.95, the corresponding estimated parameter value is considered to be an optimal result. Based on the time constant values so obtained, extended Debye model parameters, i.e., R_i and C_i of the R–C series branch, are calculated. Using the R_i and C_i values, the dissipation factor and ageing factor are calculated.

Dissipation Factor

The inefficiency of material to hold energy or behave as an insulating material is indicated by the dissipation factor. The lower the dissipation factor, the more efficient the insulator system is or the less dielectric heating. The dissipation factor is calculated using the estimated extended Debye parameters as given by (6) [24].

$$\tan\delta = \frac{\frac{1}{R_0} + \sum_{i=1}^{3} \frac{(\omega R_i C_i)^2}{R_i.(1+(\omega R_i C_i)^2)}}{\omega C_0 + \sum_{i=1}^{3} \frac{\omega C_i}{1+(\omega R_i C_i)^2}} \tag{6}$$

where R_0 is the insulation resistance, C_0 is the geometric capacitance, ω is the relaxation frequency, R_i and C_i are the resistance and capacitance of the i^{th} $R-C$ branch.

Ageing Factor

An empirical ageing factor can be used to classify the ageing condition of the XLPE cable insulation [6,14]. The ageing factor calculated from depolarisation current at time constant τ_{i+1} and τ_i is given by (7).

$$A = \frac{I_D(\tau_{i+1}) \,.\, \tau_{i+1}}{I_D(\tau_i) \,.\, \tau_i} \tag{7}$$

where τ_i is the relaxation time constant of the i^{th} $R-C$ branch, $I_D(\tau_i)$ is that part of the depolarization current characteristics due to the i^{th} $R-C$ branch.

4. RESULT AND DISCUSSION

The XLPE cable samples are aged constantly and cyclically, considering thermal and humidity stress. The Polarization–Depolarization Current (PDC) measurements are carried out on XLPE unaged and aged samples. The parameters such as the degradation index (D_I), loss factor (ϵ_r'') are estimated from the depolarization characteristics. Additional information is extracted from depolarization current characteristics to calculate the aging factor (A) and dissipation factor ($\tan\delta$) using Extended Debye model parameters. The parameters are estimated for two different charging times, i.e., 1800s and 7200s. In this section, the significant changes in the quantifying parameters are discussed.

4.1 Analysis of Depolarization Current Characteristics

Fig. 5 shows the variation of depolarization current with time for sample 1, sample 2, and sample 3 with a charging time of 1800s. It is observed that in the initial phase of depolarization, the current magnitude is low for sample 1 compared to samples 2 and 3. However, after 100s of depolarization, the current magnitude is nearly equal. The initial difference in the depolarization current magnitude is possibly due to ageing. With ageing, XLPE undergoes degradation, and particularly due to thermal stress, morphological changes may occur in the dielectric. This degradation and deterioration of the XLPE material may contribute to higher depolarization current [25]. Also, it is seen that the current magnitude in the case of sample 2 is higher than sample 3. The higher current value in sample 2 reflects more aging or degradation compared to sample 3. In case of sample 2, the RH is maintained at 50 %, whereas in sample 3, it is 80%. Due to the high RH value, the effect of thermal stress in sample 3 might have been suppressed. At higher RH values, it is expected that moisture content within the temperature–humidity-controlled chamber will be high. It may happen that the heat content due to applied thermal stress is mostly absorbed by the moisture rather than the cable insulation. Thereby reducing the thermal stress on cable insulation. Therefore, for the same temperature and ageing hours, the degradation of molecular bonds, i.e., aging is possibly less in sample 3 compared to sample 2.

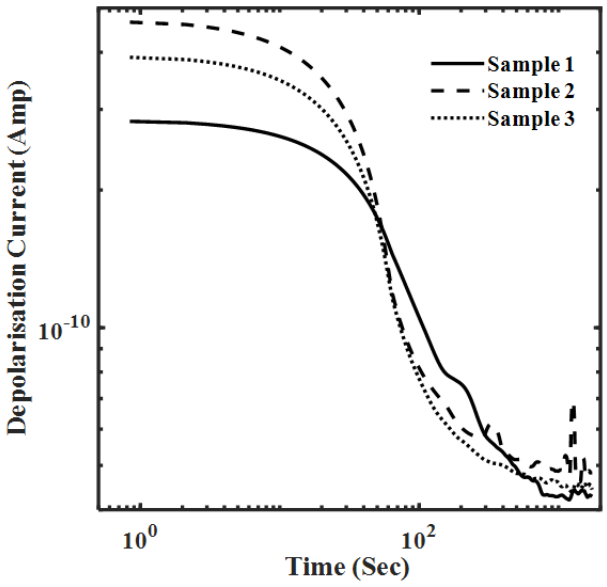

***Fig. 5**: Depolarization current variation with time for the XLPE samples 1, 2 and 3 at t_c = 1800 seconds.*

Fig. 6 shows the variation of depolarization current with time for sample 1, samples 4, and sample 5 with a charging time of 1800s. It is observed that the depolarization current magnitude is higher in samples 4 and 5 compared to sample 1. Due to the application of cyclic stress, a higher magnitude of current values is observed for aged samples. Although different RH values for samples 4 and 5 are used, the depolarization current characteristics are almost overlapping. This is possible

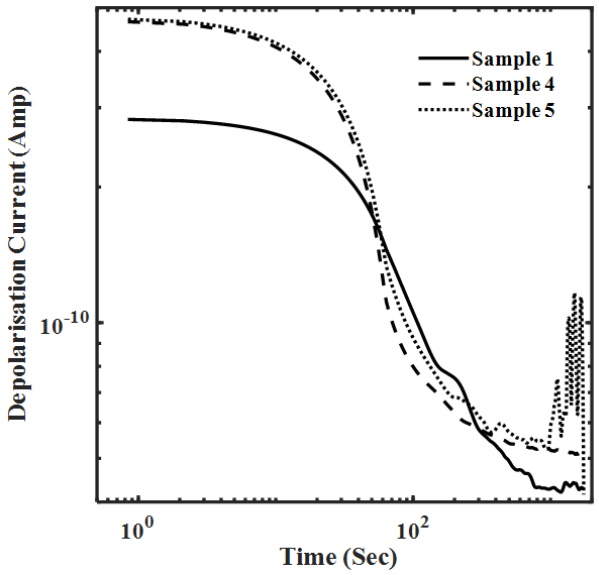

***Fig. 6**: Depolarization current variation with time for the XLPE samples 1, 4 and 5 at $t_c = 1800$ seconds.*

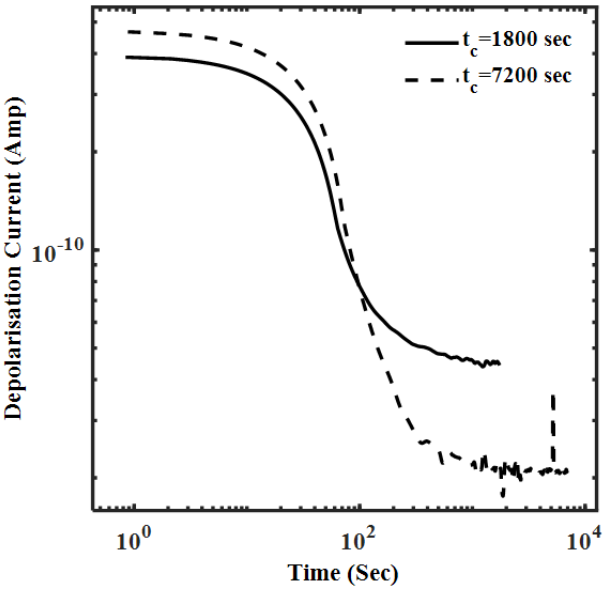

***Fig. 7**: Comparison of depolarization current response of Sample 3 for two different charging times (t_c).*

because of cyclic aging since the aging hours are less; the effect of RH is not significant, as seen with constantly aged samples.

Considering Figs. 5 and 6, it is seen that the relaxation process is prominent at the beginning and nearly similar characteristics are seen after 100 s. The depolarization current consists of capacitive charging current and absorption current. Initially, the depolarization current is the summation of both currents, but with time, exponentially decaying capacitive current vanishes and absorption current remains. The difference in depolarization characteristics before 100 s is possibly due to the difference in the capacitive current of the unaged and aged samples. However, beyond 100 s, possibly the absorption current remains nearly the same for all the samples. Therefore, it can be said that due to aging the capacitive effect of the dielectric changes, and thereby a change in the relaxation process is observed.

***Table 2**: Degradation index D_I of samples 1, 2 and 3.*

Sample Type	Q(C)	$D_I(\%)$
Sample 1	3.2044e-09	3.427
Sample 2	7.0232e-09	7.511
Sample 3	5.3639e-09	5.7365

***Table 3**: Degradation index D_I of samples 1, 4 and 5.*

Sample Type	Q(C)	$D_I(\%)$
Sample 1	3.2044e-09	3.427
Sample 4	7.3865e-09	7.8997
Sample 5	6.9277e-09	7.409

Fig. 7 shows the comparison of depolarization current in sample 3 for two different charging times, i.e., 1800s and 7200s. It is observed that depolarization current magnitude is higher for 7200s charging time compared to 1800s, within 100s of depolarization. With an increase in charging time, more polarization processes may have occurred in the dielectric, resulting in a higher density of polarized molecules, and hence depolarization current is higher initially. Due to comparatively longer polling time, relaxation processes with a higher time constant may also get completed, and hence depolarization current with lesser magnitude is observed when depolarized for 7200s beyond 100s. The difference in the current values at the start of both characteristics is 0.1 nA, whereas the difference of currents at the end of the 1800s is 0.024 nA. This shows that the difference in current at the start is more significant.

Degradation Index

To quantitatively analyze the aging effect, the degradation index of constantly and cyclically aged XLPE samples is calculated using equation 1. From the polarization–depolarization current measurement for the 1800s, the degradation index is calculated. Table 2 shows the degradation index for unaged and constantly aged samples. It is seen that with ageing the degradation index increases. This corroborates with the difference in depolarization characteristics as observed in Fig. 5 and Fig. 6. Due to aging of XLPE insulation, degradation and breakage of molecular bonds are possible and may give rise to interfacial polarization. Therefore, more polarization phenomena are expected to occur within the XLPE volume. Thus, the amount of polarized charge released as depolarization current may characterize the aging degree of the XLPE insulation. Also, from table 2, it can be observed that sample 2 has a higher degradation index compared to sample 3. This is possibly due to the RH effect.

Table 3 gives the degradation index for unaged and

***Table 4**: Comparison of Degradation index D_I of sample 3 and 4 for two different charging times (t_c).*

$t_c(sec)$	**Sample 3**	**Sample 4**
1800	5.7365	7.899
7200	7.0524	8.186

cyclically aged XLPE samples. It is observed that similar to Table 2, aged samples show a higher degradation index. Also, comparatively, sample 4 has a higher index value than sample 5, and this difference is possibly related to the difference in relative humidity. In brief, samples 2 and 4 with the low RH values give the high degradation index values when compared to the samples 3 and 5 with the high RH values. As mentioned in section 2, the degradation index provides information about the aging condition. In case of low RH value, aging is more, and therefore the degradation index value is high, whereas with high RH, ageing is less, and therefore the degradation index value is less. To understand the effect of charging time, aged XLPE samples are charged for 7200 s alongside 1800 s. Table 4 gives a comparison of the degradation index under different charging times only for samples 3 and 4. It is observed that with an increase in charging time, the degradation index value increases. During the polarization process, the charging voltage is applied for a longer time. Therefore, it is possible that more polarization charges may accumulate in the interfaces produced due to aging. As the polarization charge is more, the degradation index value increases.

Loss factor

Fig. 8 shows the loss factor (ϵ_r'') variation with frequency for the XLPE samples 1, 2, and 3. It is seen that, at 10^{-3} Hz and below, the frequency response of all the samples is similar, whereas at 10^{-3} Hz and above significant difference exist. Above 10^{-3} Hz, it is observed that sample 1, i.e., unaged XLPE, shows a low loss factor compared to samples 2 and 3, i.e., aged samples. However, sample 2, i.e., aged at RH 50 %, shows a higher loss factor compared to sample 3, i.e., aged at RH 80%. Thus relative humidity plays an important role in the aging of XLPE samples. Fig. 9 shows the loss factor (ϵ_r'') variation with frequency for the XLPE samples 1, 4, and 5. Similar to Fig. 8, here also it is observed that aged XLPE samples show a higher loss factor for the frequencies above 10^{-3} Hz. However, the loss factor of the cyclically aged samples, i.e., samples 4 and 5, overlap.

From Figs. 8 and 9, it is observed that the variation of the loss factor with frequency is different below and above at 10^{-3} Hz. As capacitive charging current vanishes from the depolarization characteristics, a change is seen between 10^{-2} and 10^{-3} Hz. Above 10^{-3} the characteristics are the summation of capacitive current and absorption current and thereby reflect the significant loss factor in unaged and aged samples. Comparing the loss factor characteristics of aged samples in Figs. 8 and 9, it is observed that a peak exists between 2 and 3 mHz. Absorption is dominant at a lower frequency and is negligible at a higher frequency. However, polarization is dominant at a higher frequency. The peak of ϵ_r'' appearing between 2 and 3 mHz is possibly due to the dominant polarization effect, which vanishes from the response in between this frequency range.

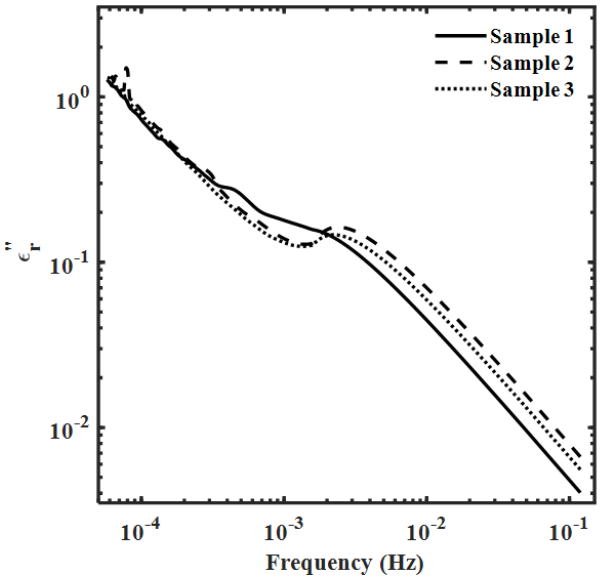

***Fig. 8**: Variation of ϵ_r'' with frequency for XLPE samples 1, 2 and 3 at $t_c = 1800$ seconds.*

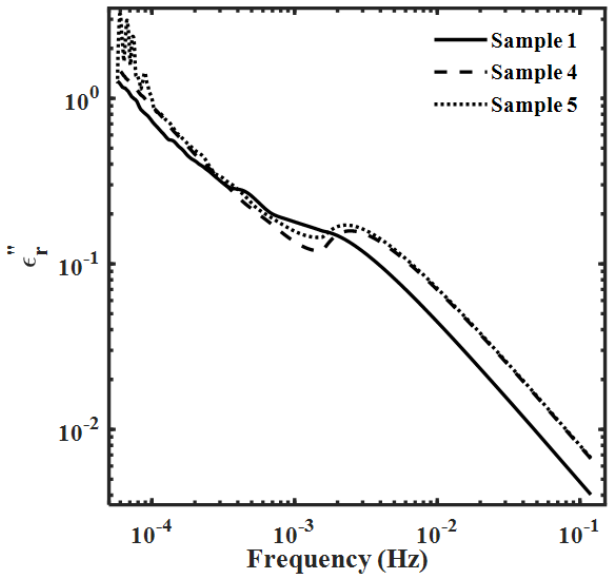

***Fig. 9**: Variation of ϵ_r'' with frequency for XLPE sample 1, 4 and 5 at $t_c = 1800$ seconds.*

Comparison of ϵ_r'' of sample 3 for two different charging times, i.e., 1800s and 7200s, are shown in Fig. 10. It is seen that the current response with higher charging time achieves a lower value of ϵ_r'' below 10^{-3} Hz. This behavior is due to longer polling time, as explained in depolarization current characteristics. Similar behavior can be observed for sample 4 in Fig. 11.

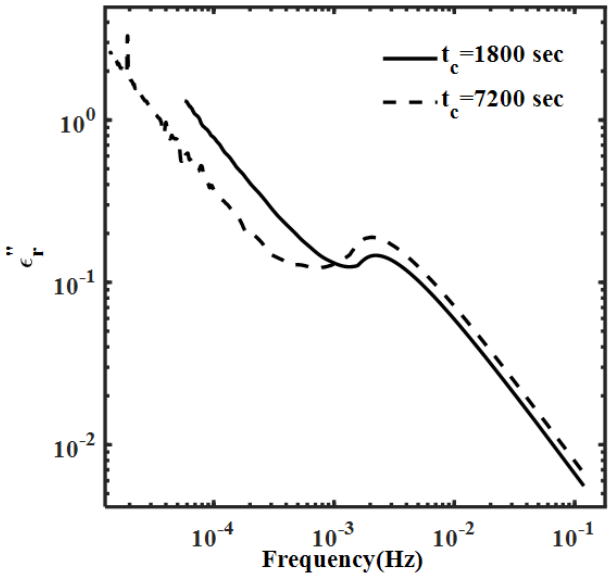

***Fig. 10**: Comparison of ϵ_r'' of sample 3 for two different charging times (t_c).*

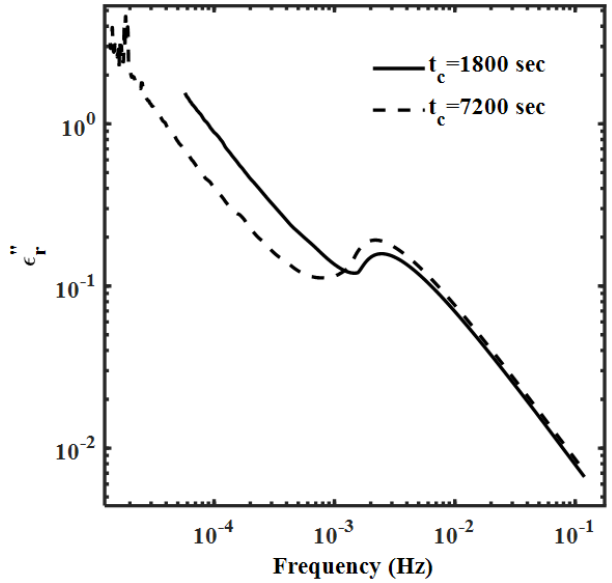

***Fig. 11**: Comparison of ϵ_r'' of Sample 4 for two different charging times (t_c).*

4.2 Analysis of Extended Debye Model Parameters

To understand the effect of ageing, dissipation factor and ageing factor are estimated using the extended Debye model. In this model, three branches are considered to represent 3 different relaxation processes. The value of pre-exponential factors a_i and corresponding time constants τ_i is obtained from curve fitting. The expression given in equations 4 and 5 is used to calculate R_i and C_i values. The value of R_0 is calculated from the polarization current data and is found to be 2 PΩ. Since XLPE is mildly aged, a considerable change in R_0 value is not observed in different samples. Table 5 shows the Debye model parameters for the charging time of 1800s

***Table 5**: Model parameters for the equivalent circuit at t_c = 1800 seconds.*

Sample	i	a_i	τ_i	$R_i(\mathrm{T\Omega})$	$C_i(nF)$
Sample 1	1	1.901e-10	24	5.26	4.56
	2	1.212e-10	120	8.25	14.54
	3	5.014e-11	8000	4.02	1990.8
Sample 2	1	8.125e-10	11.99	1.23	9.74
	2	7.706e-11	100	12.98	7.06
	3	5.333e-11	12000	2.61	4594.4
Sample 3	1	5.856e-10	9.995	1.71	5.85
	2	1.786e-10	49.99	5.59	8.93
	3	5.19e-11	9000	3.49	2576.8
Sample 4	1	8.644e-10	11.99	1.16	10.36
	2	5.789e-11	100	17.27	5.79
	3	5.706e-11	12000	2.44	4915.7
Sample 5	1	6.15e-10	12	1.63	7.38
	2	1.52e-10	60	6.58	9.12
	3	6.086e-11	8000	3.31	2416.5

***Table 6**: Ageing factor A of samples 1, 2 and 3.*

Sample Type	R-square	A
Sample 1	0.9732	12.9084
Sample 2	0.9898	28.9119
Sample 3	0.99	28.34758

at 1000 V. Calculated parameters, i.e., R_i and C_i of three different branches for five different XLPE samples are shown.

From Table 5, it is observed that model parameters modify with the aging. It can be observed that the capacitance C_3 value is higher than C_1 and C_2 values in all the cases, which is due to the higher value of τ_3. The time constant τ_3 is higher in value as the current magnitude gets saturated after a certain time, and the reduction rate of current value becomes much less. Hence the exponential term of the curve responsible for this attains a higher time constant. With a charging time of t_c=7200 seconds, the current value achieves saturation almost at the same time as with t_c=1800 seconds, due to which the current data with a lower reduction rate is very high, and hence τ_3 for t_c=7200 seconds, it attains almost ten times the higher value than with t_c=1800 seconds.

Dissipation factor

The dissipation factor of the aged and unaged XLPE samples is estimated using the parameters obtained from the extended Debye model. Fig. 12 shows the tanδ variation with frequency for XLPE samples 1, 2, and 3 at t_c = 1800 *sec*. It can be seen that sample 2 has the highest dissipation factor. Fig. 13 shows the tanδ variation with frequency for XLPE samples 1, 4, and 5 at t_c = 1800 *sec*. It can be seen that sample 4 has the highest dissipation factor. The dissipation factor is least for unaged sample 1 when compared with constant as well as cyclically aged samples. This could

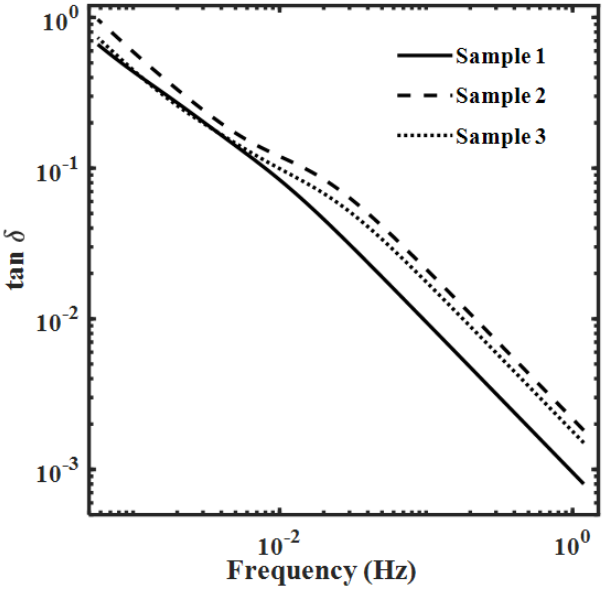

Fig. 12: $\tan\delta$ *variation with frequency for the XLPE samples 1, 2 and 3 at* $t_c = 1800$ *seconds.*

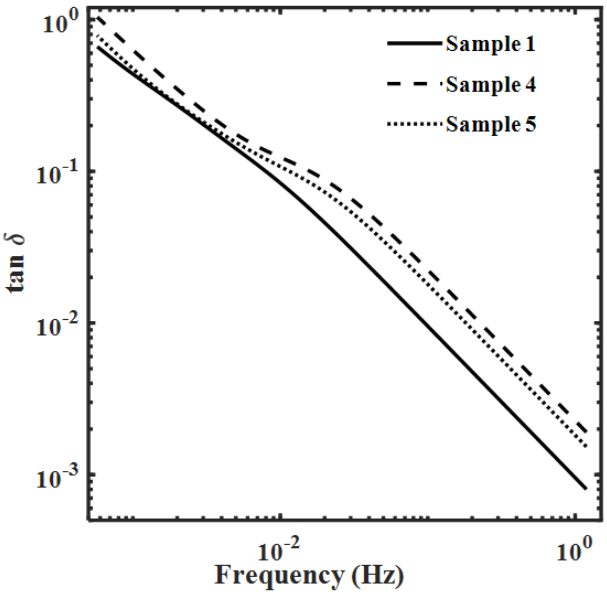

Fig. 13: $\tan\delta$ *variation with frequency for the XLPE samples 1, 4 and 5 at* $t_c = 1800$ *seconds.*

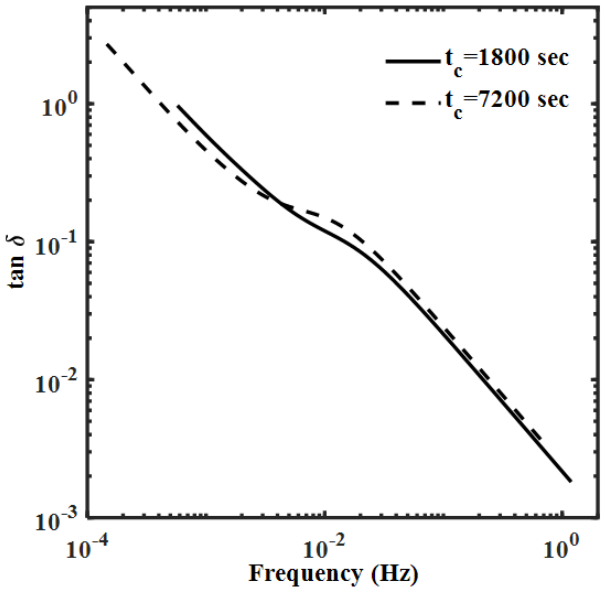

Fig. 14: *Comparison of* $\tan\delta$ *of Sample 2 for two different charging times* (t_c).

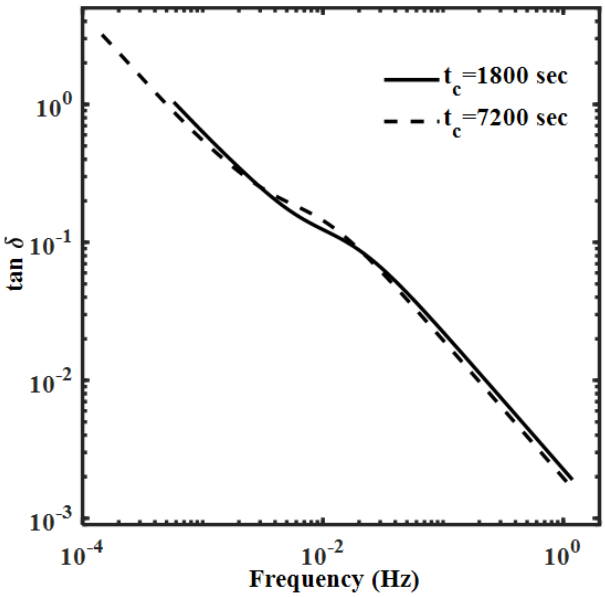

Fig. 15: *Comparison of* $\tan\delta$ *of Sample 4 for two different charging times* (t_c).

be due to higher deterioration of the samples aged with low RH than samples aged with high RH. The high RH might be obstructing the aging by reducing the effect of temperature.

Fig. 14 gives a comparison of the dissipation factor of sample 2 with two different poling times. It can be observed the curves are almost overlapping. In Fig. 15, a comparison of the dissipation factor of sample 4 at two different charging times is shown. Here also, the curves are almost overlapping. Since the charging time is varied, the polarization processes inside the insulation also change. This should result in different characteristics for the dissipation factor for the same sample with different charging times. But, since it is the case of mild aging, no considerable change was observed. In dissipation factor plots, a peak appearing between 2 and 3 mHz frequency range is observed. Similar peaks were observed in frequency transformation, which is possibly due to the vanishing of the dominant polarization effect.

Ageing Factor

The aging factor is estimated for the aged XLPE samples, according to equation 7. This parameter is estimated from the depolarization characteristics obtained

***Table 7**: Ageing factor A of samples 1, 4 and 5.*

Sample Type	R-square	A
Sample 1	0.9732	12.9084
Sample 2	0.9945	32.257
Sample 3	0.9809	24.7796

***Table 8**: Comparison of Ageing factor, A of samples 3 and 4 for two different charging times.*

$t_c(sec)$	Sample 3	Sample 4
1800	28.34758	32.257
7200	110.6	151.89

from polarization–depolarization current measurements. Table 6 gives a comparison of the aging factor (A) of the unaged sample with constantly aged XLPE samples, energized at 1000 V for 1800 s. The value of the time constants depends on fitting goodness. The R-square value shows the fitness of the curve. It is observed that with aging, the aging factor increases. Similarly, Table 7 gives a comparison of the aging factor of the unaged sample with cyclically aged samples for the same polarization–depolarization current measurement conditions. It is observed that with aging, a parameter increases. Also, it is observed from Tables 6 and 7 that XLPE samples aged at RH 50% have a higher a value compared to samples aged at RH 80%.

Table 8 gives a comparison of the aging factor, A, of samples 3 and 4, obtained with two different charging times, i.e., 1800s and 7200s. It is being observed that the aging factor is significantly higher for both the samples when polarized or energized for a longer duration. The higher value of A factor for t_c=7200 seconds is due to the higher value of τ_3. The reason for the higher τ_3 value is discussed further in the section of extended Debye model parameters.

5. CONCLUSIONS

This paper implemented the PDC method for condition assessment of XLPE cables. Accelerated aging was performed to age the XLPE samples in the laboratory, and PDC measurement was carried out. Quantifying aging parameters were studied and calculated. The parameters calculated in this paper are capable of interpreting the aging degree of the XLPE samples under consideration. The findings indicate that significant morphological changes occur in the insulation bulk due to aging, possibly associated with the phenomena of interfacial polarization. Variation of polarization processes with charging time is also discussed in this paper. Less variation of quantifying parameters from the value of the unaged sample ensures it is a case of mild aging. This work gives an understanding of the assessment method for diagnosing mildly aged XLPE cable insulation.

REFERENCES

[1] G. C. Montanari and A. Motori, "Time behavior and breakdown of XLPE cable models subjected to multiple stresses," *IEEE International Symposium on Electrical Insulation*, Toronto, ON, Canada, 1990, pp. 257-260.

[2] M. Muhr, E. Neges, R. Woschitz and C. Sumereder, "Aging behaviour of cross-linked polyethylene (XLPE) as an insulating material for high (HV)- and extra-high voltage cables (EHV)," *The 17th Annual Meeting of the IEEE Lasers and Electro-Optics Society, 2004. LEOS 2004.*, Boulder, CO, USA, 2004, pp. 232-236

[3] Q. Wang, R. Liu, S. Qin, Xi Chen, Z. Shen, Z. Hou and Z. Ju, "Insulation Properties and Degradation Mechanism for XLPE Subjected to Different Aging Periods," *CSEE Journal of Power and Energy Systems*, vol. 9, no. 5, pp. 1959-1967, Sep. 2023

[4] S. Morsalin and B. T. Phung, "Dielectric response measurement on service-aged XLPE cables: From very low frequency to power frequency," *IEEE Electrical Insulation Magazine*, vol. 36, no. 5, pp. 19-31, Sep.-Oct. 2020.

[5] E. Gulski and R. Jongen, "Condition Based Maintenance of Transmission Power Cables," *IEEE Transactions on Power Delivery*, vol. 37, no. 3, pp. 1588-1597, June 2022.

[6] B. Oyegoke, P. Hyvonen, M. Aro and Ning Gao, "Application of dielectric response measurement on power cable systems," *IEEE Transactions on Dielectrics and Electrical Insulation*, vol. 10, no. 5, pp. 862-873, Oct. 2003.

[7] V. Ďurman, M. Váry, J. Packa, J. Lelák and V. Šály, "Assessment of dielectric properties of cable insulation," *2017 18th International Scientific Conference on Electric Power Engineering (EPE)*, Kouty nad Desnou, Czech Republic, 2017, pp. 1-4.

[8] K. Zhao, M. Sun, L. Gong, H. Wang and W. Wang, "Research on Cable Aging Diagnosis Based on Short Circuit Response," *2022 4th International Conference on Power and Energy Technology (ICPET)*, Beijing, China, 2022, pp. 401-405.

[9] Huang, P.; Yu, W.; Lu, C.; He, X.; Zhang, Y.; Liu, Y.; Zhou, J.; Liang, Y, "Quantitative Evaluation of Thermal Ageing State of Cross-Linked Polyethylene Insulation Based on Polarization and Depolarization Current," *Polymers*, vol. 15, no. 5. p. 1272, 2023.

[10] Li, Y.; Peng, Z.; Xu, D.; Huang, S.; Gao, Y.; Li, Y, "Research on the Thermal Aging Characteristics of Crosslinked Polyethylene Cables Based on Polarization and Depolarization Current Measurement," *Energies*, vol. 17, no. 10, p. 2274, 2024.

[11] Küchler, E. R. Lötscher, R. Färber and C. M. Franck, "Polarization-Depolarization Current (PDC) Measurements for Volume and Surface Resistivity Analysis of Polymeric Materials," *2021 IEEE Conference on Electrical Insulation and Dielectric Phe-*

nomena (CEIDP), Vancouver, BC, Canada, 2021, pp. 17-22,

[12] K. Thungsook, P. Nimsanong, N. Marukatut and N. Pattanadech, "Polarization and Depolarization Current Measurement of Underground Cable with Different Cable lengths, Temperatures and Test Voltages," *2018 Condition Monitoring and Diagnosis (CMD)*, Perth, WA, Australia, 2018, pp. 1-4.

[13] Joshi, Abhishek and Pooja Aaradhi, "Dielectric Diagnosis of EHV current Transformer Using Frequency Domain Spectroscopy (FDS) & Polarization and Depolarization Current (PDC) Techniques," *International Journal of Scientific and Engineering Research*, vol. 3, no. 11, pp. 1 – 11, 2012.

[14] W. Li, X. Zhang, A. Zhao, L. Wu, Z. Ren, J. Deng and G. Zhang, "Studies of the polarization/depolarization current characteristics of XLPE cable," *2016 IEEE PES Asia-Pacific Power and Energy Engineering Conference (APPEEC)*, Xi'an, 2016, pp. 677-680.

[15] Ai-xuan Zhao, Long Xu, Xing Zhang, Jun-bo Deng, Guan-Jun Zhang, Xue-Feng Zhao, "Research on aging parameters of XLPE cable based on isothermal relaxation current," *AIP Advances*, vol. 8, no. 7, Jul. 2018.

[16] Y. Wang, A. Zhao, X. Zhang, Y. Shen, F. Yang, J. Deng and G. Zhang, "Study of dielectric response characteristics for thermal aging of XLPE cable insulation," *2016 International Conference on Condition Monitoring and Diagnosis (CMD)*, Xi'an, China, 2016, pp. 602-605.

[17] K. Abdolall, "Design of an accelerated aging test for polymer insulated distribution cables," *IEEE International Symposium on Electrical Insulation*, Toronto, ON, Canada, 1990, pp. 343-34.

[18] Kwan Chi Kao. *Dielectric Phenomena in Solids*, Elsevier, 2004.

[19] S. Das, J. C. Pandey and N. Gupta, "Space charge diagnostics in aged polymeric insulation," *2013 IEEE 1st International Conference on Condition Assessment Techniques in Electrical Systems (CATCON)*, Kolkata, India, 2013, pp. 395-398.

[20] S. Sulaiman, A. Mohd Ariffin, and D. T. Kien, "Determining the Number of Parallel RC Branches in Polarization / Depolarization Current Modeling for XLPE Cable Insulation", *International Journal on Advance Sciience, Engineering Information Technology*, vol. 7, no. 3, pp. 971–979, Jun. 2017.

[21] J. Raxsa, N. Phethai, M. Thanatorn and Y. Peerawut, "Determination of Dielectric Models Based on Effective Multi-Exponential Fittings," *Energies*, vol. 16, no. 12, 2023.

[22] V. Der Houhanessian. *Measurement and analysis of dielectric response in oil-paper insulation systems*, Doctoral Thesis, ETH Zurich, 1998

[23] K. Bandara, C. Ekanayake, T. Saha and H. Ma, "Investigation of moisture influence on dielectric response of ester oil impregnated pressboard," *2015 IEEE Power & Energy Society General Meeting*, Denver, CO, USA, 2015, pp. 1-5.

[24] G. Ye, H. Li, F. Lin, X. Wu, Z. Huang, Q. Zhang and J. Cai, "Study on the dielectric response characteristic of XLPE cables," *2013 Annual Report Conference on Electrical Insulation and Dielectric Phenomena*, Chenzhen, China, 2013, pp. 81-84.

[25] G. Ye, H. Li, F. Lin, J. Tong, X. Wu and Z. Huang, "Condition assessment of XLPE insulated cables based on polarization/depolarization current method," *IEEE Transactions on Dielectrics and Electrical Insulation*, vol. 23, no. 2, pp. 721-729, Apr. 2016.

Ashok Narayan Tripathi was born in Prayagraj, Uttar Pradesh, India, in 1995. He received his B. Tech in Electrical Engineering from Dr. A. P. J. Abdul Kalam Technical University, Uttar Pradesh, India and M. Tech in Power and Energy Systems from the National Institute of Technology (NIT) Meghalaya, Meghalaya, India, in 2017 and 2020, respectively. His areas of interest include high-voltage engineering, polymeric insulators and numerical techniques in electrostatics.

Supriyo Das received Master and PhD degree in Electrical Engineering from Indian Institute of Technology Madras and Indian Institute of Technology Kanpur, India respectively. He served Department of Electrical Engineering, National Institute of Technology Meghalaya, India as Assistant Professor from 2014 to 2022. Since 2022, he is working as Assistant Professor in the Department of Electrical Engineering, National Institute of Technology Jamshedpur, India. He is IEEE senior member. His research interests are statistical analysis of insulator breakdown, diagnosis and characterisation of polymeric dielectrics and lightning transients.